



# Real-Time In Situ Powder X-ray Diffraction Monitoring of Mechanochemical Synthesis of Pharmaceutical Cocrystals\*\*

Ivan Halasz, Andreas Puškarić, Simon A. J. Kimber, Patrick J. Beldon, Ana M. Belenguer, Frank Adams, Veijo Honkimäki, Robert E. Dinnebier, Bhavnita Patel, William Jones, Vjekoslav Štrukil, and Tomislav Friščić\*

Mechanosynthesis has attracted the attention of chemists and materials scientists<sup>[1]</sup> interested in new synthetic opportunities offered by a fully or nearly solvent-free reaction environment.<sup>[2–4]</sup> Recent advances in mechanochemistry<sup>[1,5]</sup> resulted from the realization that supramolecular concepts, such as molecular recognition and self-assembly,<sup>[6]</sup> templating, and (organo)catalysis<sup>[7]</sup> can be used to enhance and control mechanosynthesis. Furthermore, techniques such as liquid-assisted grinding (LAG, also solvent-drop grinding, kneading)<sup>[8]</sup> were recently developed which offered a general means to optimize mechanochemistry for quantitative and/or enantioselective synthesis. However, mechanisms of milling reactions often remain speculative and poorly understood. A persistent obstacle in this sense has been the inability to directly monitor reactions and phase changes, thereby dictating that mechanistic studies had to be performed in a stepwise fashion, that is, by stopping the milling at designated times for analysis of the reaction mixture.<sup>[9,10]</sup> Such invasive analysis is not suitable for fast reactions or for short-lived or air-sensitive intermediates. A mechanochemical process conducted in a stepwise manner can yield a different result from an uninterrupted one.<sup>[11]</sup> While temperature, pressure, and

acoustic measurements<sup>[12]</sup> have been used to follow milling reactions, such measurements are limited to specific systems.

We recently described<sup>[13]</sup> the first non-invasive, potentially general method for the real-time, in situ monitoring of milling reactions by powder X-ray diffraction (PXRD). The technique uses high-energy ( $\lambda = 0.1427 \text{ \AA}$ ,  $E = 86 \text{ keV}$ ) X-rays capable of penetrating the milling vessel, and was first used to monitor the synthesis of porous metal–organic frameworks (MOFs) from ZnO.<sup>[13,14]</sup>

In terms of X-ray scattering and mechanical behavior, organic solids provide a different set of properties than metal oxides and MOFs. Considering the importance of mechanochemistry for the screening and synthesis of pharmaceutical solids,<sup>[15,16]</sup> we now demonstrate the first real-time, in situ PXRD study of mechanochemical transformations of organic pharmaceutically relevant solids. Since the cocrystal of carbamazepine (cbz) and saccharin (sac), (cbz)(sac), is an archetypal example of a pharmaceutical cocrystal, we selected its formation as a suitable first model in our study (Figure 1 a,b).<sup>[17]</sup>

All the features in the time-resolved diffractogram obtained after neat milling (Figure 1 a) correspond to crystalline sac (CSD SCCHRN01) and the monoclinic form of cbz (CSD CBMZPN10),<sup>[18]</sup> thus indicating the absence of cocrystallization. The intensities of all the X-ray reflections diminished during milling, thus indicating amorphization, as illustrated by plotting the phase scale factor over time for cbz and sac, (Figure 1 b). This is consistent with earlier cryomilling studies that indicated amorphization by milling.<sup>[19]</sup> Rietveld analysis revealed an apparent increase in the weight content of sac during milling, thus indicating cbz is more readily amorphized (see Section 2 in the Supporting Information).

The LAG experiment, in which 50  $\mu\text{L}$  of acetonitrile were added to the reaction mixture, exhibited an entirely different X-ray intensity versus time profile (Figure 1 c). New X-ray reflections appear within 10 s of milling, accompanied by a rapid decrease in the reactant signal. The new reflections correspond to triclinic (cbz)(sac) (CSD UNEZAO).<sup>[20]</sup> Rietveld analysis of the diffractograms provided a time-resolved plot of the increase in weight fraction of the (cbz)(sac) product and reduction in the weight fractions of solid reactants cbz and sac. The disappearance of cbz and sac indicates that the LAG synthesis of a 1 mmol cocrystal (> 0.4 g) is complete within 4 min. In contrast, mechanochemical reactions of ZnO and imidazoles,<sup>[13]</sup> where effects of reactant amorphization and delayed product nucleation were observable from kinetic analysis, product formation in the

[\*] Dr. V. Štrukil, Prof. T. Friščić  
Department of Chemistry and FRQNT Centre for Green Chemistry and Catalysis, McGill University  
801 Sherbrooke St. W., H3A 0B8 Montreal (Canada)  
E-mail: tomislav.frischic@mcgill.ca

Dr. I. Halasz, A. Puškarić, Dr. V. Štrukil  
Ruđer Bošković Institute  
Zagreb (Croatia)

P. J. Beldon, Dr. A. M. Belenguer, B. Patel, Prof. W. Jones  
Department of Chemistry  
University of Cambridge, Cambridge (UK)

F. Adams, Prof. R. E. Dinnebier  
Max-Planck-Institute for Solid State Research  
Stuttgart (Germany)

Dr. S. A. J. Kimber, Dr. V. Honkimäki  
European Synchrotron Radiation Facility (ESRF)  
Grenoble (France)

[\*\*] We acknowledge R. L. Nightingale for equipment design and manufacture, D. S. Bohle for assistance in acquiring single-crystal X-ray diffraction data, A. K. Cheetham for discussions, J. K. M. Sanders for support, Herchel Smith Fund, NanoDTC Cambridge, EPSRC, NSERC Discovery Grant, FRQNT Nouveaux Chercheurs fund for funding, and the Ministry of Science, Education and Sport of the Republic of Croatia (Grant No. 098-0982904-2953).

Supporting information for this article is available on the WWW under <http://dx.doi.org/10.1002/anie.201305928>.

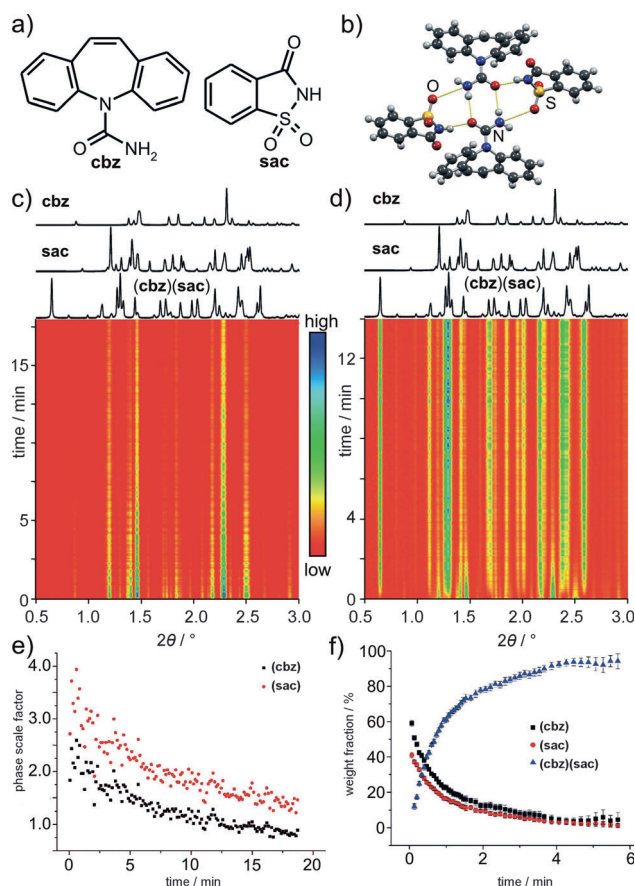


**Figure 1.** a) Reactants *cbz* and *sac*; b) a molecular assembly in *(cbz)(sac)*. Time-resolved diffractograms for: c) neat milling and d) LAG of *cbz* and *sac*. e) Time-dependent change in phase scale factors for the neat milling of *cbz* and *sac*. A drop in scale factors indicates amorphization, while the scatter of values is due to varying amounts of the sample in the X-ray beam. f) Change in the weight fraction of reactants and products in the LAG synthesis of *(cbz)(sac)*. Time-resolved diffractograms are accompanied by the simulated ones for the relevant phases of *cbz*, *sac*, and *(cbz)(sac)*.

LAG synthesis of *(cbz)(sac)* is concomitant with the disappearance of reactants. In addition to the changes in the composition of the reaction mixture, monitoring by in situ diffraction also allows the assessment of the particle sizes of the reaction components through the widths of the X-ray reflections (see Section 2 in the Supporting Information).

We next explored more complex mechanisms in the mechanosynthesis of model pharmaceutical cocrystals of nicotinamide (*na*) and suberic acid (*sub*, Figure 2a). A previous stepwise study<sup>[21]</sup> revealed that synthesis of the cocrystal *(na)<sub>2</sub>(sub)* by neat milling involves an intermediate *(na)(sub)*. The initial appearance of *(na)(sub)* was explained by the kinetically driven formation of the strong amide–carboxylic acid *R*<sub>2</sub><sup>2</sup>(8) supramolecular synthons along with carboxylic acid–pyridine *R*<sub>2</sub><sup>2</sup>(7) synthons. Further reaction gave *(na)<sub>2</sub>(sub)*, which achieves an overall greater stabilization through a larger number of weaker (amide–amide *R*<sub>2</sub><sup>2</sup>(8) and *R*<sub>2</sub><sup>2</sup>(7) pyridine–carboxylic acid) synthons. The time-resolved diffractogram (Figure 2b) from the neat milling of *na* and *sub* in a 1:1 ratio (1 mmol each) revealed the

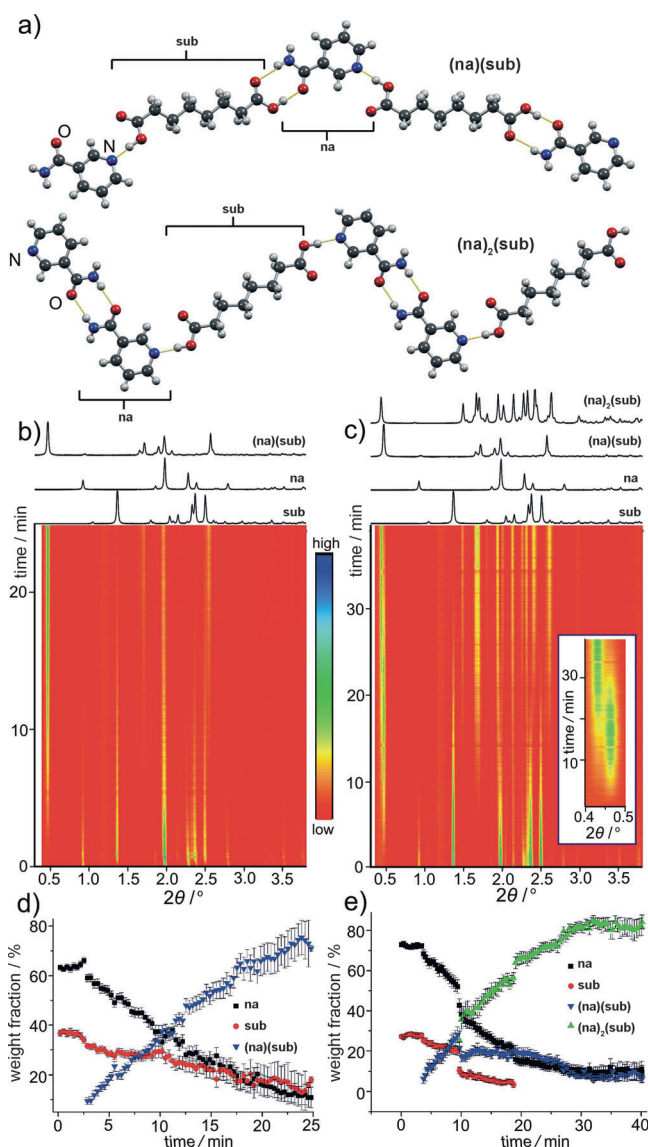


**Figure 2.** a) Fragments of hydrogen-bonded chains in the cocrystals *(na)(sub)* and *(na)<sub>2</sub>(sub)*. Time-resolved diffractograms obtained by neat milling of *na* and *sub* in stoichiometric ratios: b) 1:1 and c) 2:1. Inset in (c): enlarged region of the diffractogram between  $2\theta = 0.4^\circ$  and  $0.5^\circ$ , highlighting the initial formation of *(na)(sub)* and appearance of *(na)<sub>2</sub>(sub)*. Time-resolved diffractograms are accompanied by simulated ones for *na*,<sup>[23]</sup> *sub*,<sup>[24]</sup> *(na)(sub)*, and *(na)<sub>2</sub>(sub)*. Changes in the weight fractions of reactants and products by the neat milling of *na* and *sub* in stoichiometric ratios: d) 1:1 and e) 2:1. In (e), the sudden drop in the weight fractions of *na*, *sub*, and *(na)(sub)* after 10 min is an artefact of including *(na)<sub>2</sub>(sub)* in the refinement. The overlap of reflections of *(na)<sub>2</sub>(sub)* and *(na)<sub>2</sub>(sub)* prevents considering the presence of *(na)<sub>2</sub>(sub)* at earlier reaction times.

appearance of *(na)(sub)* within one minute, while reflections of solid *na* and *sub* disappeared over 25 min.<sup>[21,22]</sup> Rietveld analysis indicated that the formation of *(na)(sub)* proceeds at an almost constant rate (Figure 2d). Monitoring the neat milling of 2 mmol of *na* and 1 mmol of *sub* (Figure 2c) revealed the appearance of *(na)(sub)* within 1 min, followed by the formation of *(na)<sub>2</sub>(sub)*. After 40 min, the *(na)(sub)* intermediate almost completely disappeared. Quantitative

Rietveld analysis was in this case complicated by the overlap of X-ray reflections of (na)(sub) and (na)<sub>2</sub>(sub), which prevented taking into account the (na)<sub>2</sub>(sub) phase before it had built up sufficiently, approximately 10 min into the milling (Figure 2e).

We next explored the faster LAG synthesis of (na)<sub>2</sub>(sub). The time-resolved diffractogram of LAG involving 50  $\mu$ L of acetonitrile, 2 mmol na, and 1 mmol sub revealed a highly dynamic reaction environment in which the intermediate (na)(sub) (Figure 3a) disappeared within 3 min of its appearance. However, the time-resolved diffractogram also revealed

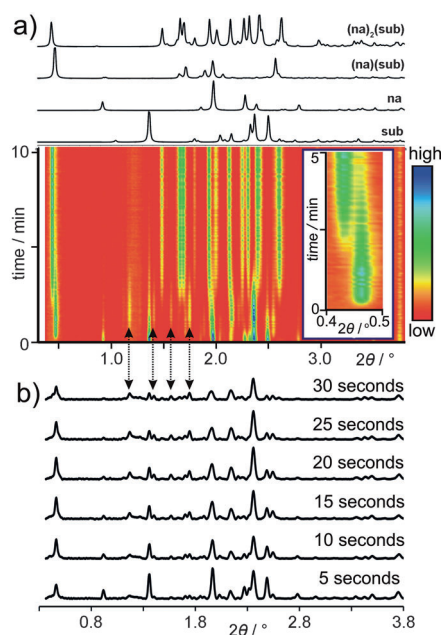


**Figure 3.** a) Time-resolved diffractogram of the LAG reaction of na and sub in a 2:1 ratio, with simulated patterns for (na)(sub), (na)<sub>2</sub>(sub), na,<sup>[23]</sup> and sub<sup>[24]</sup> shown. Inset: enlarged region of the diffractogram at  $2\theta = 0.4\text{--}0.5^\circ$ , demonstrating the formation of (na)(sub) followed by (na)<sub>2</sub>(sub). b) Diffractograms at milling times 5–30 s with characteristic reflections of **1** marked by arrows spanning (a) and (b) at  $2\theta$ :  $1.15^\circ$ ,  $1.40^\circ$ ,  $1.50^\circ$  and  $1.75^\circ$ . All other features in (b) are explained by phases (na)(sub), na, and sub.

four transient reflections (Figure 3a,b) between about 15 s and 4 min which could not be assigned to na, sub, (na)(sub), or (na)<sub>2</sub>(sub). The appearance and disappearance of these reflections was concomitant with that of (na)(sub) and we assume they correspond to an intermediate crystalline phase (**1**) not seen in neat milling experiments. To confirm that **1** is not an artefact of in situ studies, we attempted to reproduce it under conventional laboratory conditions by stopping the reaction after 1, 2, and 5 min. Indeed, **1** was detected in the reactions after 1 and 2 minutes, after minimizing the time for sample isolation and preparation. The PXRD pattern of a sample milled for 1 min collected on a laboratory instrument using CuK $\alpha$  radiation exhibited signals of na, sub, and (na)(sub), but also reflections at  $2\theta$  angles of  $12.6^\circ$ ,  $15.2^\circ$ ,  $17.0^\circ$ , and  $18.9^\circ$ , which are consistent with  $d$  spacings for **1** observed using the in situ technique at  $3.52\text{ \AA}$ ,  $2.95\text{ \AA}$ ,  $2.64\text{ \AA}$ , and  $2.37\text{ \AA}$ , respectively. Laboratory CuK $\alpha$  radiation

also resolved a low-angle reflection of **1** ( $2\theta = 5.30^\circ$ ,  $d = 8.35\text{ \AA}$ ) which could not be distinguished in the in situ measurements from a low-angle reflection of (na)(sub) (Figure 4). The same reflections appeared by LAG with CH<sub>3</sub>CN or CH<sub>3</sub>NO<sub>2</sub>, thus suggesting that **1** is not a solvate. The reflections of **1** disappeared upon aging, which demonstrates that (na)(sub) and **1** are separate intermediates rather than one phase that structurally resembles (na)(sub).

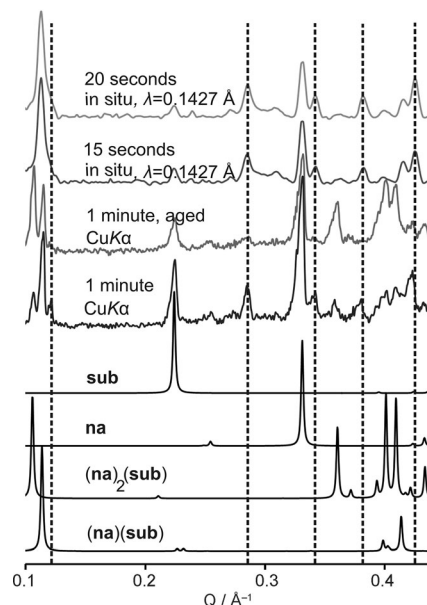


**Figure 4.** X-ray diffractograms collected for the LAG reaction of na and sub by using the in situ technique ( $\lambda = 0.1427\text{ \AA}$ ) after 15 s and 20 s milling, compared to diffractograms collected using CuK $\alpha$  radiation ( $\lambda = 1.54056\text{ \AA}$ ) on a sample of the reaction mixture after 1 min milling that had been either freshly extracted or left to age in air. Simulated patterns for na,<sup>[23]</sup> sub,<sup>[24]</sup> (na)(sub), and (na)<sub>2</sub>(sub) are also shown. Data are plotted on a  $Q$  scale ( $Q = 1/d$ ). Dotted lines highlight four discernible reflections of **1** and a fifth one that is observable using CuK $\alpha$  radiation, but seen in in situ studies as a shoulder.

In summary, we have reported the first real-time, in situ X-ray diffraction study of mechanochemical synthesis and transformations of organic cocrystals. With time resolution in seconds, this technique allows the identification and monitoring of neat and liquid-assisted milling reactions, as well as in situ assessment of changes in the size of crystalline particles. While mechanochemical transformations of inorganic substances often last for hours or days,<sup>[25]</sup> the in situ technique demonstrated a surprising speed for LAG cocrystallization, and yielded almost 0.5 g of the pharmaceutical cocrystal of carbamazepine and saccharin in 4 min. This method also revealed a previously unseen intermediate in the LAG cocrystallization of nicotinamide and suberic acid. Our results demonstrate both kinetic and thermodynamic control over product formation in essentially a solid-state environment, and paint a dynamic picture that would normally be expected for solution reactions. The in situ monitoring technique thus has the potential to further our understanding of milling reactions, and especially of fast liquid-assisted



grinding. Rietveld analysis using the current setup is complicated by a combination of the very short X-ray wavelength with position-sensitive detectors without analyzer crystals, as well as a relatively thick, unevenly distributed<sup>[9,12]</sup> sample. We are developing means to improve this new technique.

## Experimental Section

Experiments were conducted at the European Synchrotron Radiation Facility (ESRF) beamline ID15B in a modified MM200 Retsch mill operating at 30 Hz. Each reaction was conducted in a 14.5 mL Perspex jar with one stainless-steel ball (7 mm diameter). Incident X-rays were selected using a bent Laue Si crystal, with a beam size on the sample of 300  $\mu\text{m}^2$ . Diffracted X-rays were detected on a flat-panel Pixium charge-coupled detector, and diffractograms obtained by summing 10 or less detector frames (each collected over 0.4 s, giving a time resolution of 4 s). The background was subtracted using the Sonneveld–Visser algorithm in Powder3D.<sup>[26]</sup> Rietveld<sup>[27]</sup> refinement was performed with Topas (version 4.2). Laboratory PXRD experiments were carried out on a Bruker D2 Phaser with Ni-filtered CuK $\alpha$  radiation. (na)(sub): monoclinic, space group  $P2_1/c$ ,  $Z = 4$ ,  $a = 4.967(5)$ ,  $b = 35.16(4)$ ,  $c = 8.88(1)$  Å,  $\beta = 93.98(1)^\circ$ ,  $V = 1547(3)$  Å<sup>3</sup>, 3434 independent reflections ( $R_{\text{int}} = 0.0547$ ).  $R_1 = 0.0688$  ( $I > 2\sigma(I)$ ), 0.1295 (all data).  $wR(F^2) = 0.1696$  ( $I > 2\sigma(I)$ ), 0.2093 (all data),  $S = 1.029$ . (na)<sub>2</sub>(sub): triclinic, space group  $P\bar{1}$ ,  $Z = 1$ ,  $a = 5.035(1)$ ,  $b = 5.500(1)$ ,  $c = 18.968(4)$  Å,  $\alpha = 88.025(2)^\circ$ ,  $\beta = 86.707(2)^\circ$ ,  $\gamma = 89.457(2)^\circ$ ,  $V = 524.0(2)$  Å<sup>3</sup>, 2370 independent reflections ( $R_{\text{int}} = 0.0303$ ).  $R_1 = 0.0610$  ( $I > 2\sigma(I)$ ), 0.1067 (all data).  $wR(F^2) = 0.1499$  ( $I > 2\sigma(I)$ ), 0.1864 (all data),  $S = 1.101$ . CCDC 949090 ((na)(sub)) 949091 ((na)<sub>2</sub>(sub)) contain the supplementary crystallographic data for this paper. These data can be obtained free of charge from The Cambridge Crystallographic Data Centre via [www.ccdc.cam.ac.uk/data\\_request/cif](http://www.ccdc.cam.ac.uk/data_request/cif).

Received: July 8, 2013

Published online: September 23, 2013

**Keywords:** cocrystals · mechanochemistry · pharmaceutical materials · reaction monitoring · X-ray diffraction

- [1] a) S. L. James, P. Collier, I. Parkin, G. Hyatt, D. Braga, L. Maini, W. Jones, C. Böhm, A. Krebs, J. Mack, D. Waddell, W. Shearouse, A. G. Orpen, C. J. Adams, T. Friščić, J. W. Steed, K. D. M. Harris, *Chem. Soc. Rev.* **2012**, *41*, 413; b) P. Baláž, M. Achimovičová, M. Baláž, P. Billik, Z. Cherekzova-Zheleva, J. M. Criado, F. Delogu, E. Dutková, E. Gaffet, F. J. Gotor, R. Kumar, I. Mitov, T. Rojac, M. Senna, A. Streletskii, K. Wiczorek-Ciurawa, *Chem. Soc. Rev.* **2013**, *42*, 7571; c) A. Stolle, T. Szuppa, S. E. S. Leonhardt, B. Ondruschka, *Chem. Soc. Rev.* **2011**, *40*, 2317.
- [2] a) G. A. Bowmaker, N. Chaichit, C. Pakawatchai, B. W. Skelton, A. H. White, *Dalton Trans.* **2008**, 2926; b) V. Štrukil, M. D. Igrc, M. Eckert-Maksić, T. Friščić, *Chem. Eur. J.* **2012**, *18*, 8464; c) C. B. Aakeröy, P. C. Chopade, *Org. Lett.* **2011**, *13*, 1; d) R. Thorwirth, A. Stolle, B. Ondruschka, A. Wild, U. S. Schubert, *Chem. Commun.* **2011**, 47, 4370.
- [3] F. Schneider, T. Szuppa, A. Stolle, B. Ondruschka, H. Hopf, *Green Chem.* **2009**, *11*, 1894.
- [4] a) G. A. Bowmaker, *Chem. Commun.* **2013**, 49, 334; b) T. Friščić, S. L. Childs, S. A. A. Rizvi, W. Jones, *CrystEngComm* **2009**, *11*, 418.
- [5] Besides reactions by milling or grinding, mechanochemistry also includes single-molecule mechanochemistry and sonochemistry: J. Ribas-Arino, D. Marx, *Chem. Rev.* **2012**, *112*, 5412.
- [6] a) K. Užarević, I. Halasz, I. Đilović, N. Bregović, M. Rubčić, D. Matković-Čalogović, V. Tomišić, *Angew. Chem.* **2013**, *125*, 5614; *Angew. Chem. Int. Ed.* **2013**, *52*, 5504; b) M. Pascu, A. Ruggi, R. Scopelliti, K. Severin, *Chem. Commun.* **2013**, 49, 45.
- [7] a) A. Bruckmann, A. Krebs, C. Bolm, *Green Chem.* **2008**, *10*, 1131; b) D. A. Fulmer, W. C. Shearouse, S. T. Medonza, J. Mack, *Green Chem.* **2009**, *11*, 1821.
- [8] a) T. Friščić, A. V. Trask, W. Jones, W. D. S. Motherwell, *Angew. Chem.* **2006**, *118*, 7708; *Angew. Chem. Int. Ed.* **2006**, *45*, 7546; b) D. Braga, M. Curzi, A. Johansson, M. Polito, K. Rubini, F. Grepioni, *Angew. Chem.* **2006**, *118*, 148; *Angew. Chem. Int. Ed.* **2006**, *45*, 142.
- [9] a) K. D. M. Harris, *Nat. Chem.* **2013**, *5*, 12–14; b) I. A. Tumanov, A. F. Achkasov, E. V. Boldyreva, V. V. Boldyrev, *CrystEngComm* **2011**, *13*, 2213.
- [10] a) M. R. Caira, L. R. Nassimbeni, A. F. Wildervanck, *J. Chem. Soc. Perkin Trans. 2* **1995**, 2213; b) X. Liu, G. Liu, H. Zhao, Z. Zhang, Y. Wei, M. Liu, W. Wen, Z. Zhou, *J. Phys. Chem. Solids* **2011**, *72*, 1245.
- [11] a) V. Štrukil, L. Fábíán, D. G. Reid, M. J. Duer, G. J. Jackson, M. Eckert-Maksić, T. Friščić, *Chem. Commun.* **2010**, 46, 9191; b) I. A. Tumanov, A. F. Achkasov, E. V. Boldyreva, V. V. Boldyrev, *Russ. J. Phys. Chem. A* **2012**, *86*, 1014.
- [12] a) L. Takacs, *Prog. Mater. Sci.* **2002**, *47*, 355; b) F. K. Urakaev, V. V. Boldyrev, *Powder Technol.* **2000**, *107*, 93.
- [13] T. Friščić, I. Halasz, P. J. Beldon, A. M. Belenguer, F. Adams, S. A. J. Kimber, V. Honkimäki, R. E. Dinnebier, *Nat. Chem.* **2012**, *5*, 66.
- [14] P. J. Beldon, L. Fábíán, R. S. Stein, A. Thirumurugan, A. K. Cheetham, T. Friščić, *Angew. Chem.* **2010**, *122*, 9834; *Angew. Chem. Int. Ed.* **2010**, *49*, 9640.
- [15] a) A. Newman, *Org. Process Res. Dev.* **2013**, *17*, 457; b) C. C. Sun, *Expert Opin. Drug Delivery* **2013**, *10*, 201; c) N. J. Babu, A. Nangia, *Cryst. Growth Des.* **2011**, *11*, 2662; d) D. R. Weyna, T. Shattock, P. Vishweshwar, M. J. Zaworotko, *Cryst. Growth Des.* **2009**, *9*, 1106.
- [16] a) A. Delori, T. Friščić, W. Jones, *CrystEngComm* **2012**, *14*, 2350; b) T. Friščić, W. Jones, *J. Pharm. Pharmacol.* **2010**, *62*, 1547; c) P. Sanphui, S. S. Kumar, A. Nangia, *Cryst. Growth Des.* **2012**, *12*, 4588.
- [17] P. Vishweshwar, J. A. McMahon, M. L. Peterson, M. B. Hickey, T. R. Shattock, M. J. Zaworotko, *Chem. Commun.* **2005**, 4601.
- [18] Crystal-structure data were retrieved from the Cambridge Structure Database (CSD), version 5.34 (November 2012) + 1 update.
- [19] a) C. Maheshwari, A. Jayasankar, N. A. Khan, G. E. Amidon, N. Rodríguez-Hornedo, *CrystEngComm* **2009**, *11*, 493; b) A. Jayasankar, A. Somwangthanaroj, Z. J. Shao, N. Rodríguez-Hornedo, *Pharm. Res.* **2006**, *23*, 2381.
- [20] S. G. Fleischman, S. S. Kuduva, J. A. McMahon, B. Moulton, R. D. Bailey Walsh, N. Rodríguez-Hornedo, M. J. Zaworotko, *Cryst. Growth Des.* **2003**, *3*, 909.
- [21] S. Karki, T. Friščić, W. Jones, *CrystEngComm* **2009**, *11*, 470.
- [22] The crystal structures of (na)<sub>2</sub>(sub) and (na)(sub) were re-determined from room-temperature single-crystal X-ray diffraction data.
- [23] L. Fábíán, N. Hamill, K. S. Eccles, H. A. Moynihan, A. R. Maguire, L. McCausland, S. E. Lawrence, *Cryst. Growth Des.* **2011**, *11*, 3522.
- [24] V. R. Thalladi, M. Nüsse, R. Boese, *J. Am. Chem. Soc.* **2000**, *122*, 9227.
- [25] G. Štefanić, S. Krehula, I. Štefanić, *Chem. Commun.* **2013**, DOI: 10.1039/C3CC44803G.
- [26] B. Hinrichsen, R. E. Dinnebier, M. Jansen, *Z. Kristallogr.* **2006**, Supplement 23, 231.
- [27] H. M. Rietveld, *J. Appl. Crystallogr.* **1969**, *2*, 65.